Computation of Annual Strike Probability of a Wind-borne Tumbling Missile using TOMAXI

Yuzuru Eguchi*[a], Soichiro Sugimoto[a], Yasuo Hattori[a], Takahiro Murakami[a] and Hiromaru Hirakuchi[a]

[a] Central Research Institute of Electric Power Industry, Abiko, JAPAN

Abstract: A numerical example of annual strike probability of a tornado-borne missile is presented in the paper, using a compact numerical scheme. The scheme is composed of two steps. First, trajectories of wind-borne missiles are computed by TONBOS (ver.4) where wind field of a tornado is modeled by the Fujita model (DBT-77) with a proposed velocity fluctuation model. The missiles located in various positions on the ground or in air are assumed to initially take random orientation, and to be injected into the wind field. After injection, missiles in air are also assumed to take random orientation. The annual strike probability is computed using TOMAXI with a prescribed tornado wind hazard curve as well as trajectory data produced by TONBOS (ver.4), assuming that tornadoes around a site concerned have uniform probability with respect to the path direction. The computational results allow us to estimate the spatial distribution of annual strike probability of a missile for a horizontal or vertical plate of unit area.

Keywords: Tornado missile, Annual strike probability, Random orientation, Computer simulation.

1. INTRODUCTION

Gigantic Tsunami waves inundated the Fukushima-Daiichi Nuclear Power Plant site on 11th of March, 2011, and triggered the severe accidents; the core melt-downs of the three BWR plants. The Nuclear Regulation Authority of Japan (NRA) established after the accident has issued the New Regulatory Requirements for Nuclear Power Plants in 2013, part of which newly demands integrity against tornado. According to the Assessment Guide for Tornado Effect on Nuclear Power Plants [1] published by NRA, safety-related facilities of a nuclear power plant should be sound against tornado-borne missiles as well as against tornado wind loads and pressure change loads. Some design tornado missile speeds for 100m/s of maximum tornado wind speed are listed as examples in the Assessment Guide. The missile speeds are comparable to or beyond those listed in the U.S. regulatory guide, NUREG 1.76 [2], as seen in **Fig.1.**

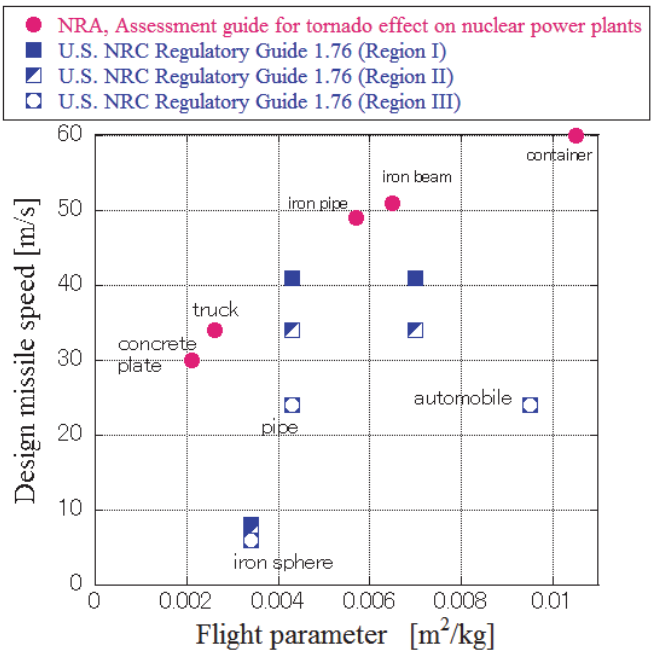

Fig.1 Design tornado missile speeds listed in regulatory guides in USA and Japan

On the other hand, significance of tornado in Japan is much less than that of USA in general. One of the examples is the annual death tolls from 1961 to 2017 caused by tornadoes shown in **Fig.2**. Considering such a difference of tornado impacts between Japan and USA, we can infer that the design missile speeds shown in the Assessment Guide for Tornado Effect on Nuclear Power Plants [1] could be very conservative. The reasons of such possibly excessive conservatism may have twofold. First reason is because the maximum tornado wind speed of Japan is set based on the Fujita scale (F-

* corresponding author: eguchi@criepi.denken.or.jp

scale), while that is based on the Enhanced Fujita scale (EF-scale) in U.S. For example, wind speed range of F3 is 162-209 mph in terms of 3-second gust speed, while that of EF-scale is 138-167 mph. Second reason is because the design missile speeds of the U.S. NUREG 1.76 are set by partially considering probabilistic aspect of tornado-borne missile strike on a safety-related SSC (Structure, System or Component) [3], [4]. On the other hand, the design missile speeds shown in the Assessment Guide published by NRA is based on deterministic approach [5]. The probabilistic approach considered in the U.S. NUREG 1.76 can be justified by the fact that probability of missile strike damage in SSC, P_{dam}, can be expressed by the product of probabilities of several sequential events such as;

$$P_{dam} = P_1 P_2 P_3 P_4 P_5 P_6 \quad (1)$$

where P_1 is probability of tornado attack on a site, P_2 is probability of existence and availability of missile in a site, P_3 is probability of injection of a missile into tornado, P_4 is probability of suspension and flight of a missile, P_5 is probability of missile flight orientation toward an SSC concerned, and P_6 is probability of damage upon missile strike of an SSC.

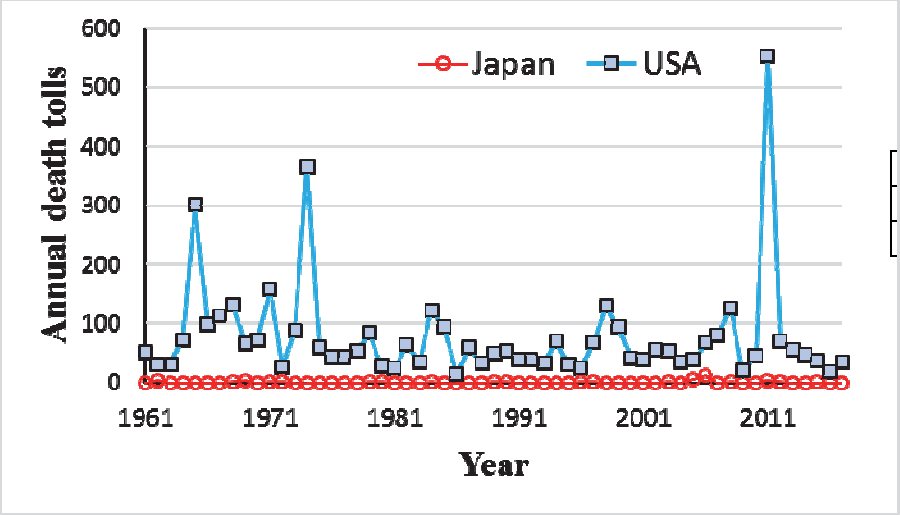

country	Japan	USA
average	0.7	77.4
median	0	53

Fig.2 Annual death tolls caused by tornadoes in USA and Japan

In previous studies regarding probability of missile strike damage, Twisdale *et al.* [6] and EPRI [7], [8] developed TORMIS to compute tornado missile strike probability. Hope *et al.* [9] developed TMSC (Tornado Missile Strike Calculator) using Excel-based user-interface. One of the common features of the two codes is that tornadoes are generated randomly in accordance with prescribed probability distribution of tornado intensity and path direction, and the other is the missile injection and flight are numerically simulated using the Monte Carlo method. On the other hand, Goodman and Koch estimated the tornado missile strike probability using the Green's function [10-12], postulating that tornado missile transport is a diffusion Markovian process. In their paper [10], they presumed that the average Green's function satisfies the condition of axial symmetry due to randomization over thousands of tornado histories, being non-uniform in the vertical direction due to the gravitational field. In our previous paper [13], we employed the idea rather similar to the assumption employed by Goodman and Koch [10], assuming that tornadoes to attack a site do not have any preferential direction along their paths. The proposed evaluation method was applied for the annual probability of tornado missile strike on a tall slender structure [13]. This method has been further extended to compute annual strike probability of a wind-borne missile possibly hitting a horizontal plate and a vertical plate locating in an arbitrary point in space [14]. In the extended computer code, named as TOMAXI, it is assumed that tornadoes (or straight wind) around a site concerned have uniform probability with respect to the path direction (or straight wind direction). This assumption allows us to reduce the computational efforts in evaluating the annual missile strike probability for a horizontal or vertical plate. For the details of the assumption and the numerical formulation of TOMAXI, readers should be referred to our previous paper [14].

In our previous studies [13], [14], we used the trajectories of missiles which were computed using a deterministic model, TONBOS (ver.3). In the present study, we use the probabilistic trajectory data produced by TONBOS (ver.4) to compute the annual strike probability of a missile for a horizontal and vertical plate. In TONBOS (ver.4), wind field of a tornado is modeled by the Fujita model (DBT-77) with assumed velocity fluctuation. Furthermore, a missile is assumed to initially take random orientation and to be injected into the wind field by aerodynamic and gravitational forces. If a missile is initially placed on the ground, the lift force due to ground effect is considered in addition to the lift force due to upward cross-flow. The dynamic motion of a missile in flight is modeled with three-dimensional translational equations with imposing aerodynamic drag, lift and side forces as well as gravity force. Tumbling of a missile is modeled by the random orientation model where the aerodynamic drag, lift and side forces are computed using the formulae derived from the cross-flow theory in a way similar to Twisdale *et al.* [6]. The physical model of TONBOS (ver.4) was validated by comparing the numerical results and an experimental observation of trajectories of a rod released in a straight wind.

In the following section, we explain theoretical background of the probabilistic missile motion model employed in TONBOS (ver.4). In Section 3, a numerical example of annual missile strike probability is presented using the proposed method with the probabilistic trajectory data. Section 4 is devoted to the conclusion of the present paper.

2. THEORETICAL BACKGROUND

2.1. Outline of the Computational Flow

Figure 3 shows the flow of the proposed computational scheme for the annual missile strike probability. Missile flight trajectories of missiles initially placed at various positions relative to tornado path are computed by TONBOS. Each trajectory can be related to local wind speed, V, of the missile initially sitting at a specific local point relative to the tornado position and moving direction. Missile strike probability per unit area of a target at position (r, z), $q(r,z)$, is computed by TOMAXI for each local wind speed bin. On the other hand, annual exceedance probability of local wind speed, $H(V)$, can be computed by a tornado hazard analysis code, such as TOWLA (Tornado Wind Speed Hazard Model for Limited Area) [15]. The probability density function, $P(V)$, with respect to local wind speed is obtained by the partial differentiation of $H(V)$ with respect to V. Finally, we can obtain annual probability of tornado-borne missile strike on a target of unit area with the convolutional integration of product of $q(r,z)$ and $P(V)$ over V.

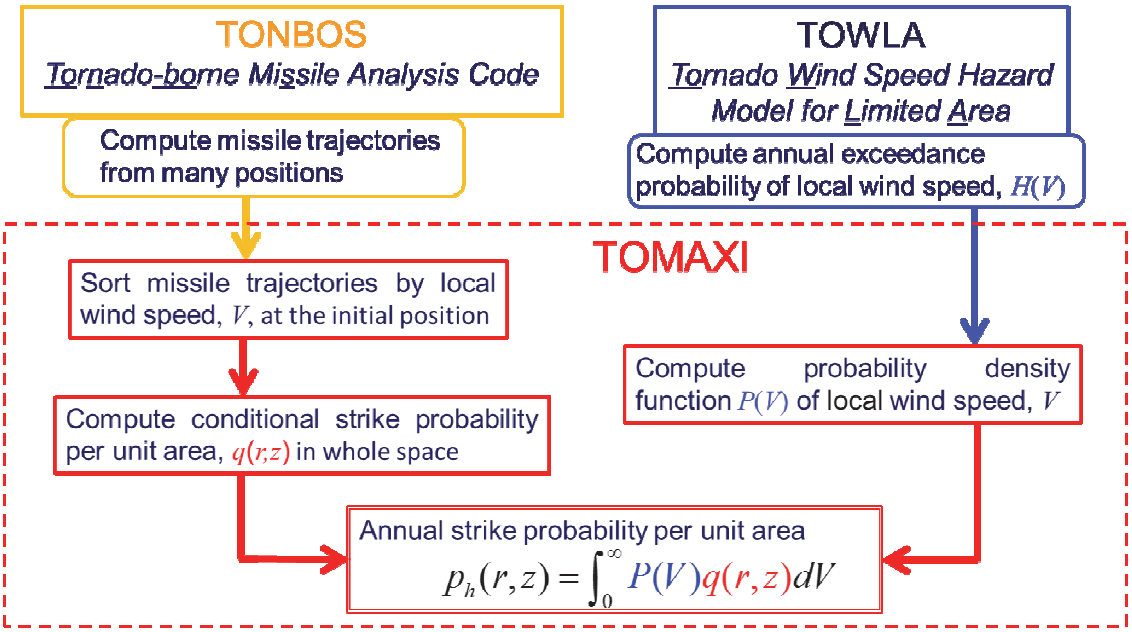

Fig.3 Computational flow of annual strike probability using TONBOS, TOWLA and TOMAXI

2.2. Aerodynamic Forces

The aerodynamic drag, lift and side forces are computed using the formulae derived from the cross-flow theory in a way similar to Twisdale and Vickery[16] and Twisdale *et al.* [6]. The three-dimensional vector of the aerodynamic force, **f**, is expressed as follows for a rectangular missile shown in **Fig.4**.

$$\mathbf{f} = \frac{1}{2}\rho|\mathbf{W}-\mathbf{V}|^2 Ld\left(C_D\mathbf{v}_{re} + C_L\mathbf{q} + C_S\mathbf{s}\right) \quad (1)$$

where the variables denotes the following.

$\mathbf{f}=(f_x, f_y, f_z)$: aerodynamic force, ρ : air density, $\mathbf{W}$: wind velocity,
$\mathbf{V}=(u,v,w)$: missile velocity, $\mathbf{W}-\mathbf{V}$: relative wind velocity,
$\mathbf{v}_{re}$: unit relative wind velocity (in drag direction), $\mathbf{q}$: unit vector in lift direction,
$\mathbf{s}$: unit vector in side-force direction, C_D : drag coefficient of a rectangular missile,
C_L : lift coefficient of a rectangular missile, C_S : side-force coefficient of a rectangular missile,
Ld : maximum surface area of a rectangular missile

The directions of drag, lift and side forces ($\mathbf{v}_{re}$, **q** and **s**) are shown in **Fig.5** as an example. The unit vectors are formally defined as follows with longitudinal vector, **L**, along the largest length of the rectangular missile.

$$\mathbf{v}_{re} = \frac{\mathbf{W}-\mathbf{V}}{|\mathbf{W}-\mathbf{V}|} \quad (2a), \qquad \mathbf{s} = \frac{\mathbf{L}\times\mathbf{v}_{re}}{|\mathbf{L}\times\mathbf{v}_{re}|} \quad (2b), \qquad \mathbf{q} = \mathbf{v}_{re}\times\mathbf{s} \quad (\because \ |\mathbf{v}_{re}\times\mathbf{s}| = 1) \quad (2c)$$

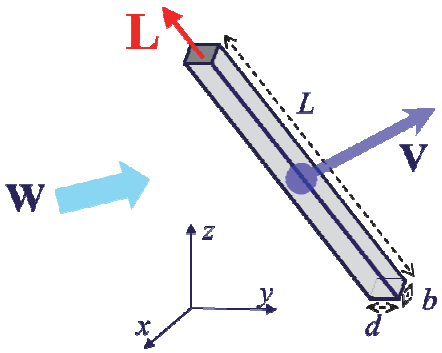

Fig. 4 Wind and missile velocity vectors

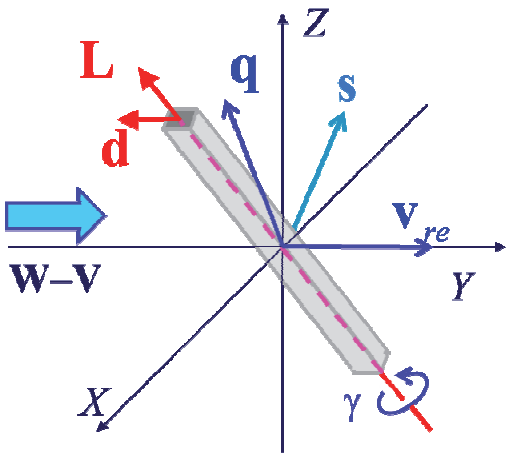

Fig. 5 Drag, lift and side force directions ($\mathbf{v}_{re}$, **q and **s**)**

Drag coefficient, lift coefficient and side-force coefficient of a rectangular missile can be calculated by the formulae shown in Eqs.(3a) to (3c), based on the cross-flow theory in a way similar to the formulae employed by Twisdale and Vickery [16] and Twisdale *et al.* [6].

$$C_D = \frac{b}{L}C_{bd}\left|\cos^3\alpha\right| + C_{Ld}\left|\cos^3\gamma\right|\sin^3\alpha + \frac{b}{d}C_{Lb}\left|\sin^3\gamma\right|\sin^3\alpha \quad (3a)$$

$$C_L = C_{Ld}\left|\cos\gamma\sin\alpha\right|^2\left|\cos\gamma\right|\cos\alpha - \frac{b}{L}C_{bd}\left|\cos\alpha\right|\cos\alpha\sin\alpha + \frac{b}{d}C_{Lb}\left|\sin^3\gamma\right|\sin^2\alpha\cos\alpha \quad (3b)$$

$$C_S = C_{Ld}\cos\gamma\left|\cos\gamma\right|\sin\gamma\sin^2\alpha - \frac{b}{d}C_{Lb}\sin\gamma\left|\sin\gamma\right|\cos\gamma\sin^2\alpha \quad (3c)$$

In the above formulae, α denotes angle of attack of relative wind vector for the longitudinal vector, **L**, as shown in **Fig.6**. Angle γ denotes angle of between side-force vector, **s**, and lateral vector, **d**, along the second largest length of the rectangular missile. In other words, lateral vector, **d**, can be produced by rotating the vector, **s**, by γ around the longitudinal vector, **L**, with the following formula.

$$\mathbf{d}=\begin{pmatrix} q_0^2+q_1^2-q_2^2-q_3^2 & 2(q_1q_2-q_0q_3) & 2(q_1q_3+q_0q_2) \\ 2(q_1q_2+q_0q_3) & q_0^2-q_1^2+q_2^2-q_3^2 & 2(q_2q_3-q_0q_1) \\ 2(q_1q_3-q_0q_2) & 2(q_2q_3+q_0q_1) & q_0^2-q_1^2-q_2^2+q_3^2 \end{pmatrix}\mathbf{s} \qquad (4)$$

In the above, q_0, q_1, q_2 and q_3 are unit quaternions defined below with the longitudinal vector, **L**= (L_x, L_y, L_z).

$$q_0=\cos\frac{\gamma}{2}\ ,\ q_1=\frac{L_x}{|\mathbf{L}|}\sin\frac{\gamma}{2}\ ,\ q_2=\frac{L_y}{|\mathbf{L}|}\sin\frac{\gamma}{2}\ ,\ q_3=\frac{L_z}{|\mathbf{L}|}\sin\frac{\gamma}{2} \qquad (5)$$

In Eqs. (3a) to (3c), C_{Ld}, C_{Lb} and C_{db} are drag coefficients of the rectangular missile for wind right to each face as shown in **Fig.7**. The values employed are C_{Ld}=C_{Lb}=1.2 and C_{db}=2.0, as suggested by Maruyama et al. [17]. Twisdale and Vickery [16] took the drag coefficients to be consistent with static wind tunnel experiments. However, we do not so because such drag coefficients have turned out too large to reproduce dynamic the flight behavior shown in Section 2.7.

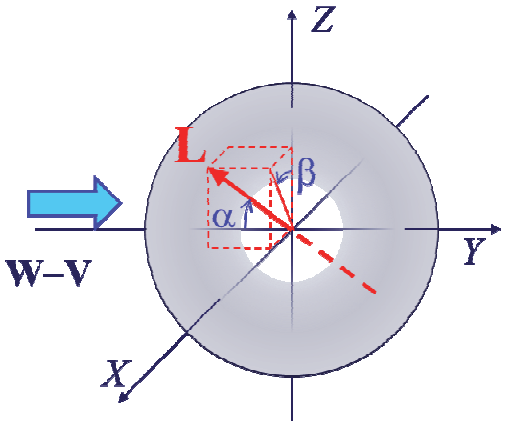

Fig. 6 Missile orientation with reference to relative wind

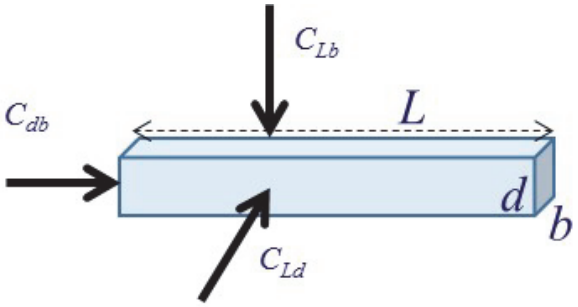

Fig. 7 Definition of drag coefficients for wind right to each face

2.3. Random Orientation

Orientation of a missile in air is altered in a variable interval using angles ψ, ϕ and γ with respect to the relative wind vector, $\mathbf{v}_{re}$ as defined in **Fig.8**. The angles ψ, ϕ and γ are selected using random numbers, ξ_1, ξ_2 and ξ_3, ranging from 0 to unity in a way similar to Twisdale and Vickery [16] and Twisdale *et al.* [6], as follows.

$$\psi=\cos^{-1}(1-2\,\xi_1) \qquad (6a)$$

$$\phi=\pi(2\,\xi_2-1) \qquad (6b)$$

$$\gamma=2\pi\xi_3 \qquad (6c)$$

Angle of attack, α, is related to angles ψ and ϕ, as $\alpha=\cos^{-1}(\cos\phi\sin\psi)$, and the longitudinal vector, **L**, can be expressed as follows.

$$\mathbf{L}=(\sin\phi\,\sin\psi,\ -\cos\phi\,\sin\psi,\ \cos\psi) \qquad (7)$$

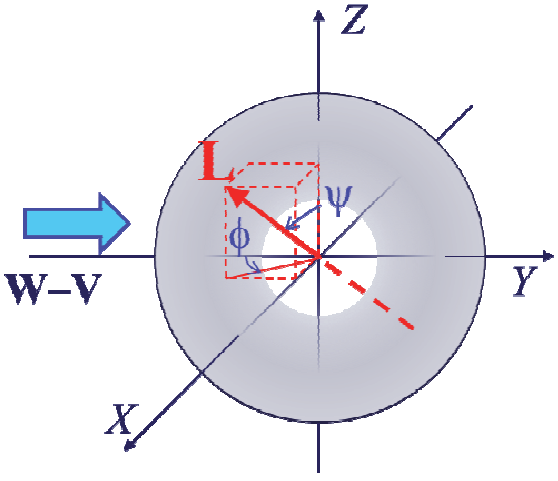

Fig. 8 Orientation of missile main axis defined with ψ and ϕ

In the model of Twisdale and Vickery [16] and Twisdale *et al.* [6], the orientation is altered at fixed frequency. In the present model, on the other hand, the orientation is altered whenever an increment of the representative missile rotation angle, θ, numerically computed from the hypothetical rotational equation below, reaches π.

$$\frac{\partial^2\theta}{\partial t^2} = k\frac{[C_D A]}{m}\frac{\rho|\mathbf{W}-\mathbf{V}|^2}{L} \tag{8}$$

where k is a constant and $[C_D A]$ is a flight parameter defined as below;

$$[C_D A] = \frac{C_{Ld}Ld + C_{Lb}Lb + C_{db}db}{3} \tag{9}$$

Equation (8) is supposed to mimic one degree-of-freedom rotational equation below, under the assumption that I and $C_M A$ are proportional to mL^2 and $[C_D A]$, respectively.

$$I\frac{\partial^2\theta}{\partial t^2} = \frac{1}{2}C_M A\rho|\mathbf{W}-\mathbf{V}|^2 L \tag{10}$$

where I, A, and C_M denote moment of inertia, representative area and moment coefficient, respectively.

2.4. Injection Model

Initial orientation of missiles can be set either uniformly or randomly in the present model. The aerodynamic drag, lift and side forces are computed using the formulae (1) according to the initial orientation of the missiles. Furthermore, a missile on and near the ground is assumed to be subject to lift force, $\mathbf{f}_L$, generated by asymmetric air flow around an object due to the ground effect [18]. Denoting the magnitude of the horizontal component of the relative wind velocity vector, by $|\mathbf{W}-\mathbf{V}|_{x,y}$, we have modeled the lift force due to ground effect, $\mathbf{f}_L$, by the following relation.

$$\mathbf{f}_L = \lambda_r\frac{1}{2}\rho[C_D A]|\mathbf{W}-\mathbf{V}|_{x,y}^2 f(Z/d) \tag{11a}$$

$$f(Z/d) = \frac{1-Z/3d}{1+Z/d} \tag{11b}$$

$$Z = z_c - d/2 \tag{11c}$$

where d is a representative missile height, and z_c is the elevation of the object center from the ground level. The proportional constant, λ_r, takes value from zero to unity, depending on the aerodynamic property of a missile, while λ_r=1 is good for a deterministic model [19], [20] to maintain conservatism.

2.5. Fluctuating Wind Field Model

In the model of Twisdale and Vickery [16] and Twisdale *et al.* [6] and in our previous missile flight simulation model [19], [20], any wind fluctuation is not considered at all. In the present probabilistic model, on the other hand, we assume that tornado wind velocity, $\mathbf{W}$, probabilistically fluctuates around and along the mean velocity $\mathbf{W}_m$ as below.

$$\mathbf{W} = \mathbf{W}_m + \Delta\mathbf{W}(\xi_a + \xi_b - 1) \tag{12}$$

where ξ_a and ξ_b are independent random numbers selected from uniform range from zero to unity, while $\mathbf{W}_m$ and $\Delta\mathbf{W}$ are defined as follows using wind velocity derived from the Fujita model [21] at the point, $\mathbf{W}_{Fujita}$.

$$\mathbf{W}_m = \frac{1}{G_{3s}}\mathbf{W}_{Fujita} \tag{13}$$

$$\Delta\mathbf{W} = (G_{\max} - 1)\mathbf{W}_m = \frac{G_{\max} - 1}{G_{3s}}\mathbf{W}_{Fujita} \tag{14}$$

In the above equations, G_{3s} is a 3-second gust factor, and $G_{\max}$ is a ratio of maximum value, $|\mathbf{W}_m+\Delta\mathbf{W}|$, against mean value, $|\mathbf{W}_m|$. In the present model, the random numbers, ξ_a and ξ_b, are associated with each missile and are updated when the missile orientation is updated. The probability distribution, p_W, for the velocity magnitude, $W=|\mathbf{W}|$, is characterized by a hut function as shown in **Fig.9**, which can be formally written using $W_m=|\mathbf{W}_m|$ and $\Delta W=|\Delta\mathbf{W}|$ as follows.

$$p_W(W) = \begin{cases} \dfrac{W - W_m}{\Delta W^2} + \dfrac{1}{\Delta W} & (W_m - \Delta W < W < W_m) \\ -\dfrac{W - W_m}{\Delta W^2} + \dfrac{1}{\Delta W} & (W_m < W < W_m + \Delta W) \\ 0 & (otherwise) \end{cases} \tag{15}$$

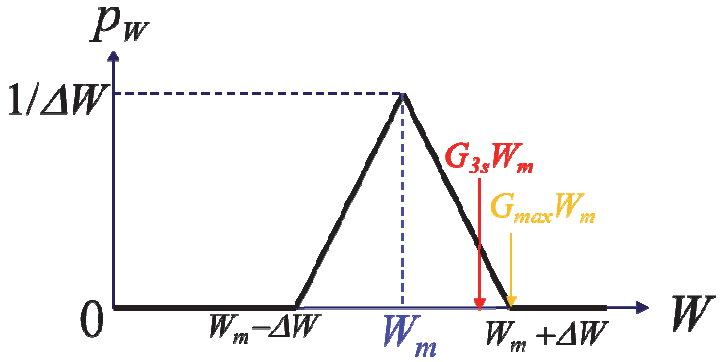

Fig.9 Probability distribution, p_W, of each velocity component

2.6. Fight Model & Time Integration Scheme

The translational motion of a missile is assumed to be governed by the Newton's second law with gravitational force and aerodynamic force, $\mathbf{f}=(f_x, f_y, f_z)$ given by Eq. (1), such that;

$$m\frac{du}{dt} = f_x \quad (16a), \qquad m\frac{dv}{dt} = f_y \quad (16b), \qquad m\frac{dw}{dt} = f_z - mg \quad (16c)$$

where m is mass of missile, and g is gravitational acceleration. The time-integration for Equations (16a) to (16c) is performed in an explicit manner such as,

$$\mathbf{V}(t+\Delta t) = \mathbf{V}(t) + \frac{\partial \mathbf{V}(t)}{\partial t}\Delta t \tag{17a}$$

$$\mathbf{X}(t+\Delta t) = \mathbf{X}(t) + \mathbf{V}(t)\Delta t + \frac{\partial \mathbf{V}(t)}{\partial t}\frac{\Delta t^2}{2} \tag{17b}$$

where $\mathbf{X}(t)$ is the position of a missile at time, t, and Δt is the time increment. If both $\mathbf{X}(t)$ and $\mathbf{V}(t)$ are known, the time derivative of $\mathbf{V}(t)$ can be computed via Equations (16a) to (16c), because tornado wind velocity $\mathbf{W}$ at a missile position at t can be computed with equations (13) to (15). Therefore, all terms in the right-hand side of equations (16a) to (16c) become known if both $\mathbf{X}(t)$ and $\mathbf{V}(t)$ are known, allowing the position and the velocity of a missile at $t=T+\Delta t$ to be computed easily. This means that time integration can be conducted sequentially if one gives the initial condition of the position and the velocity of a missile at $t=0$.

Equation (8) is similarly integrated in time as below.

$$\omega(t+\Delta t) = \omega(t) + \frac{\partial^2\theta}{\partial t^2}\Delta t \tag{18a}$$

$$\theta(t+\Delta t) = \theta(t) + \omega\Delta t + \frac{\partial^2\theta(t)}{\partial t^2}\frac{\Delta t^2}{2} \tag{18b}$$

2.7. Validation of Aerodynamic & Fight Model

A wind tunnel experiment conducted by Lin [22] at Texas Tech University was selected as a reference to validate the present aerodynamic and flight model. In the wind tunnel experiment, 4 kinds of rods were released with varying initial angle of attack under straight wind condition. The flight trajectories captured with a video camera were processed and compiled in terms of $K\bar{x}$ versus $K\bar{t}$, where non-dimensional horizontal displacement, $\bar{x}$, is defined as $gx/|\mathbf{W}|^2$ with horizontal dimensional displacement, x, while non-dimensional time, $\bar{t}$, is defined as $gt/|\mathbf{W}|$ with time, t. Non-dimensional quantity, K, is called Tachikawa number, which is defined as $K=\rho|\mathbf{W}|^2Ld/2mg$. Since the non-dimensional values, $K\bar{x}$, as function of $K\bar{t}$ are similar among the 4 kinds of rods as shown in **Fig.10 (a)**, the present numerical model has been applied to a rod whose specifications are as follows; L=381.0mm, d=12.7mm, b=6.4mm, m=0.0179kg. The other computational conditions are set as tabulated in **Table 1**. In the numerical simulation, about 40,000 rods with random initial orientations are released from 10m height in the uniform horizontal wind field without fluctuation. **Figure 10 (b)** shows the discrete non-dimensional values, $K\bar{x}$, as function of $K\bar{t}$, which agree well with those of the Lin's experiment as a whole.

Uncertainty in the simulation results could be due to the drag coefficients, C_{Ld}, C_{Lb} and C_{db}, and the constant, k, in Eq. (8), because these values are not based on strict physical background. If the drag coefficients have been increased, the rod would fly farther in wind direction. If the constant, k, has been increased, the rod orientation would be altered less frequently and the variation of the flight distance would be increased (the scatter of plot in **Fig.10(b)** would be widened more). Nevertheless, these values listed in Table 1 seems to be well-suited for the present benchmark test.

Table 1 ; Computational conditions for reproduction of Lin's wind tunnel experiment

symbol	$\|\mathbf{W}\|$	C_{Ld}	C_{Lb}	C_{db}	ρ	g	Δt	k
unit	m/s	-	-	-	kg/m^3	m/s^2	s	-
value	15	1.2	1.2	2.0	1.226	9.80665	0.001	1.0

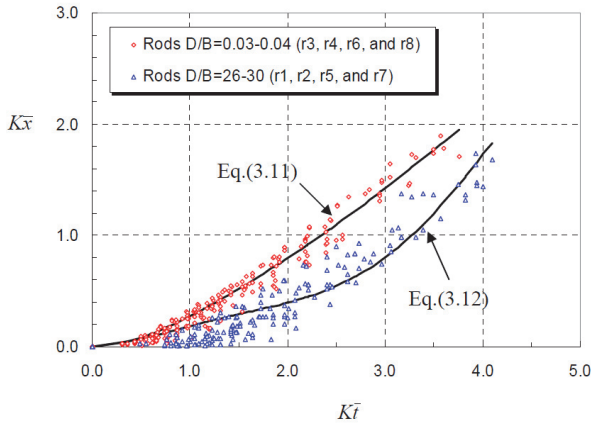

Fig. 10(a) Experimental results by Lin [22]

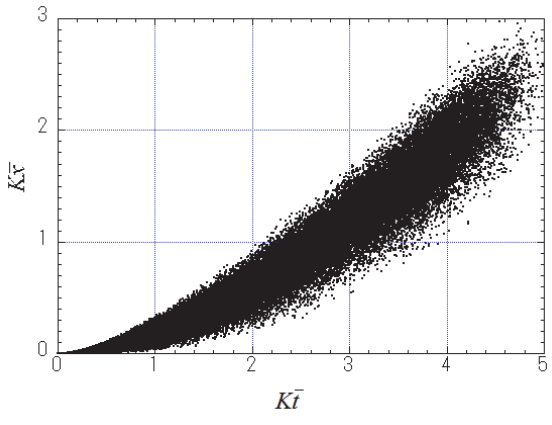

Fig. 10(b) Numerical results by the present model

3. ANNUAL STRIKE PROBABILITY

3.1. Computational Conditions

Annual strike probabilities of an automobile on a perpendicular plate and a horizontal plate of unit area are computed as a numerical example using TONBOS(ver.4) and TOMAXI. The annual exceedance probability of the local wind speed at a certain point, $H(V)$, is hypothetically assumed as $H(V)=0.00152\exp(-0.10466V)$, which takes $H(V)=10^{-6}$/year at V=70m/s and $H(V)=10^{-7}$/year at V=92m/s. We have assumed that the mass of an automobile is 1,140kg and the dimensions are 4.4m (length) x 1.7m (width) x 1.5m (height). Tornado condition is set using the design tornado of Region I in NUREG1.76 [2] such that the maximum wind speed of tornadoes is set at 103m/s (maximum tangential speed:81m/s, translational speed:21m/s) and the core radius, R_m, is 45.7m for the Fujita wind field model. The gust factors, G_{3s} and G_{max} are set at 1.2 and 1.3, respectively. The proportional constant, λ_r, for ground effect in Eq. (11a) is set at 0.5. Automobiles are placed as potential missiles at 50,049 (243 by 243) points within a $4R_m$ x $4R_m$ square region ahead of the initial tornado position. Then, the trajectories of missiles are computed with TONBOS(ver.4) using the proposed probabilistic injection/flight model. **Figure 11** shows a snapshot of the missile motions driven by the counterclockwise tornado traveling in the x direction.

Figure 12 (a) shows the maximum horizontal speed of each automobile indicated by colour at each initial position, while **Fig. 12 (b)** shows the horizontal displacement of each automobile expressed similarly. **Figure 13 (a)** shows cumulative probability distribution of maximum horizontal speeds of 50,049 (243 by 243) automobiles, while **Fig. 13 (b)** shows that of horizontal displacements. The largest value of the maximum horizontal speeds is 38.06m/s among 50,049 (243 by 243) automobiles, while that of horizontal displacement is 74.1m. Almost flat gradient of the cumulative probability curve near the upper bound suggests that the chance of such large values of automobile speed and displacement is extremely small.

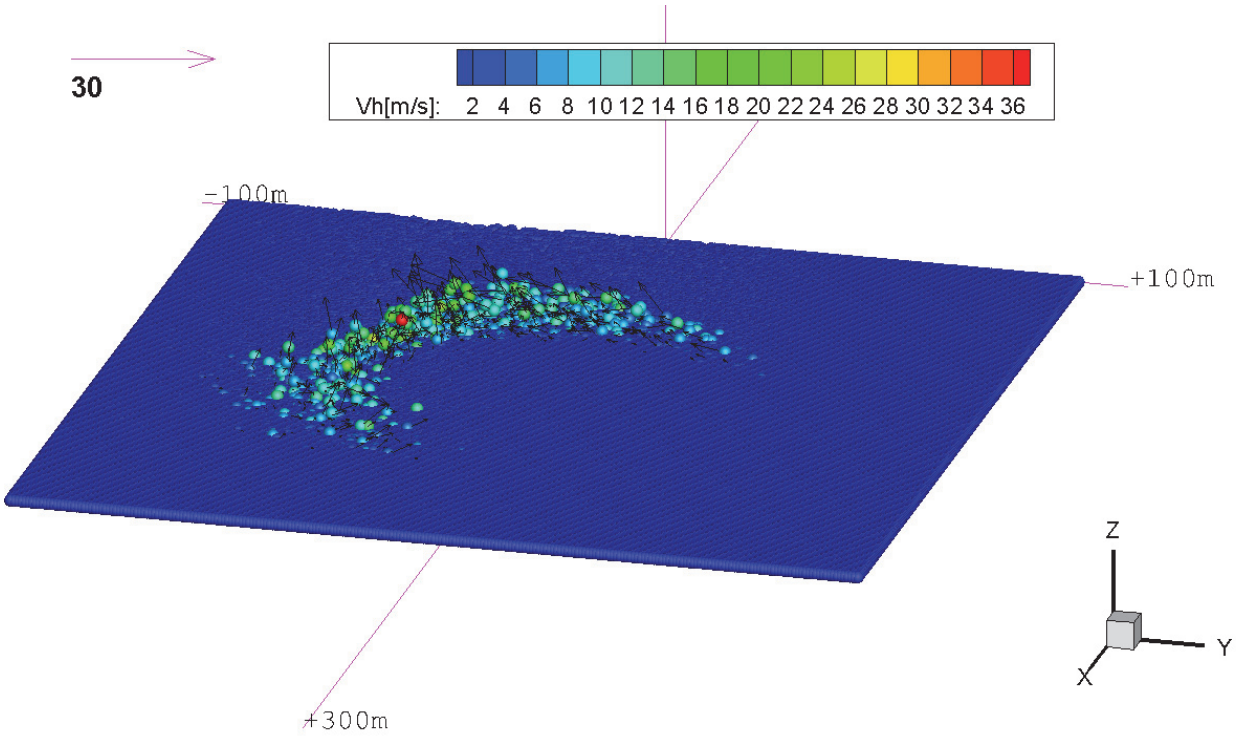

Fig.11 Snapshot of automobile positions and velocity vectors (Color corresponds to horizontal automobile speed, Vh)

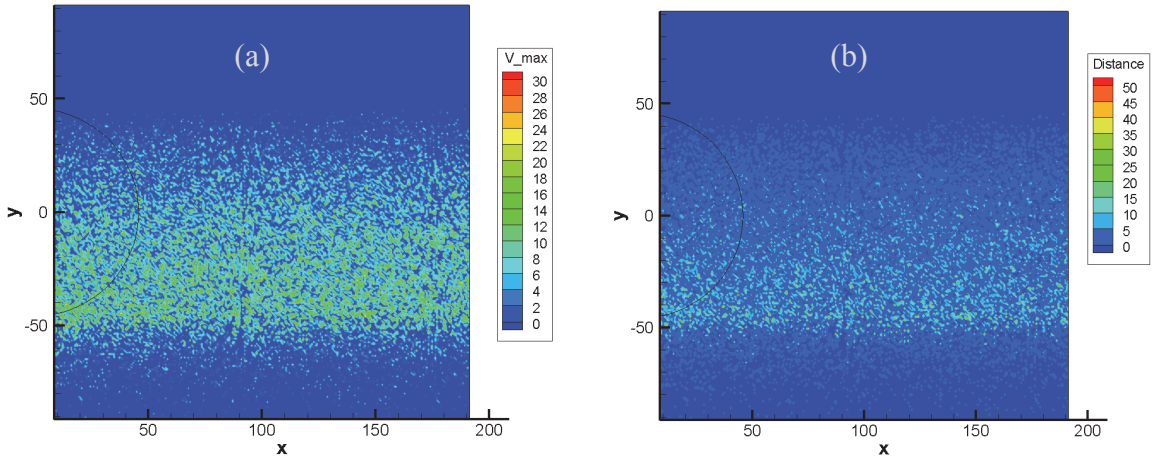

Fig.12 Maximum horizontal speed (a) and flight displacement distance (b) of an automobile depicted with color at the original position [unit: m/s and m, respectively]

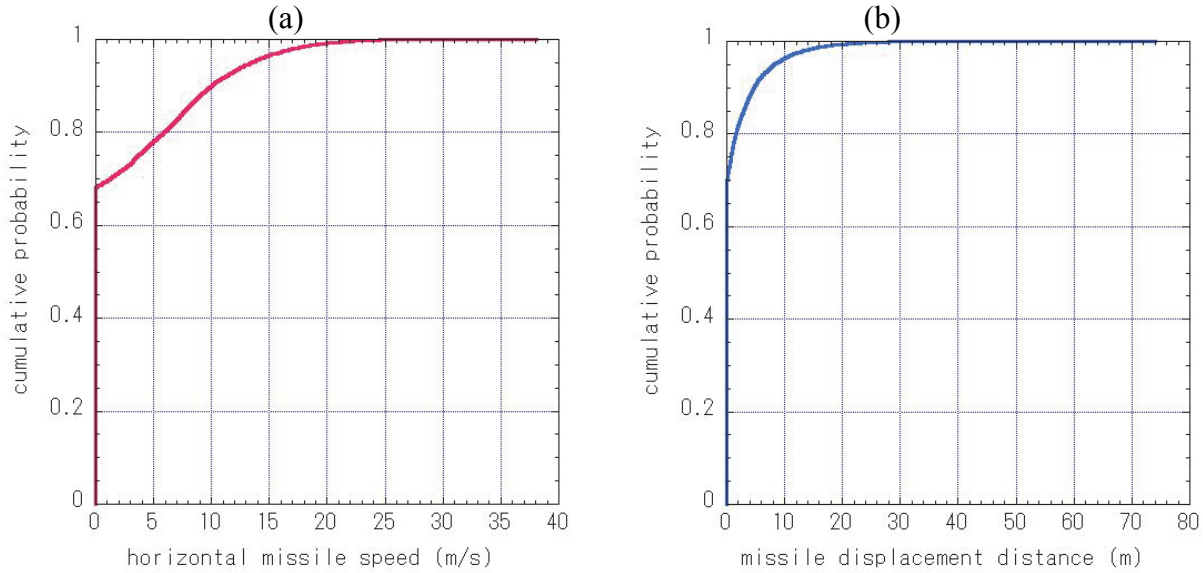

Fig.13 Cumulative probability of maximum horizontal speed (a) and flight displacement distance (b) of 243x243 automobiles

3.2. Computational Results

The trajectory results computed with TONBOS(ver.4) are used in TOMAXI to compute the conditional automobile strike probability for a horizontal plate and a vertical plate of unit area. The annual probability of tornado-borne automobile strike on a target of unit area is obtained with the convolutional integration of product of the conditional automobile strike probability and the prescribed wind speed density function over whole wind speed range. **Figure 14 (a)** shows computed spatial distribution the annual probability of tornado-borne automobile strike on a horizontal plate per $1m^2$ in common logarithm, while **Fig. 14 (b)** shows that of a vertical plate per unit area. These figures indicate that strike probability is relatively high in the vicinity of an initial automobile position and decreases as the distance between the initial automobile position and a target location. It is also seen in **Fig. 14 (a)** that the automobile strike probability on the horizontal plate almost vanished above z=3m where the horizontal component of automobile velocity is dominant.

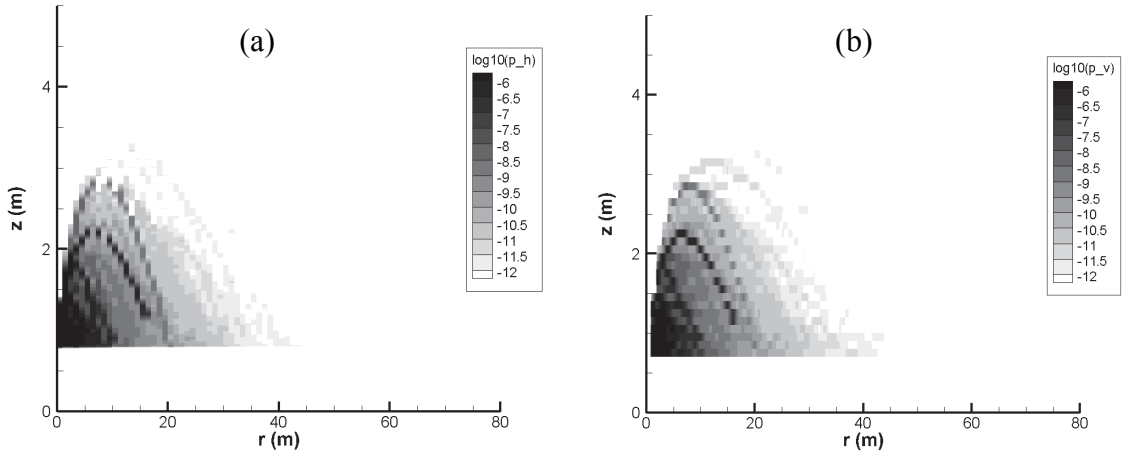

Fig.14 Annual automobile strike probability for a horizontal (a) and vertical (b) plate

4. CONCLUSION

Compact computational schemes of the spatial distribution of annual strike probability of a tornado-borne missile is presented in the paper. As an example, annual strike probability of an automobile on the ground under EF5 tornado condition has been demonstrated. The velocity fluctuation model and random orientation model are mainly explained in the present paper, which are newly implemented in TONBOS (ver.4) to take the probabilistic features into account. Such probabilistic trajectory data produced by TONBOS (ver.4) are used to compute the annual strike probability using TOMAXI with prescribed tornado wind hazard curve. The present work has demonstrated that the proposed scheme paves way to a compact and simple assessment of annual strike probability of wind-borne missile, if uniform probability with respect to the path direction (or straight wind direction) is justifiable presumption.

References

[1] Nuclear Regulation Authority of Japan, “Assessment Guide for Tornado Effect on Nuclear Power Plants”, June 2013.
[2] U.S. Nuclear Regulatory Commission, “Regulatory Guide 1.76, Design-Basis Tornado and Tornado Missiles for Nuclear Power Plants”, Revision 1, March 2007.
[3] Antaki, G., “Protection of Nuclear Power Plants from Tornado Missiles”, Becht Engineering Blog, 2015. (https://becht.com/blog/protection-of-nuclear-power-plants-from-tornado-missiles)
[4] Simiu, E. and Scanlan, R. H., “Wind Effects on Structures: Fundamentals and Applications to Design”, 3rd Edition, John Wiley & Sons, Hoboken, NJ, 1996.
[5] Maruyama, T., “Simulation of flying debris using a numerically generated tornado-like vortex”, Journal of Wind Engineering and Industrial Aerodynamics, vol.99(4), pp.249-256, 2011.
[6] Twisdale, L.A., Dunn, W.L. and Davis, T.L., “Tornado Missile Transport Analysis”, Nuclear Engineering and Design, **51**, 295-308, 1979.
[7] EPRI, “Tornado Missile Simulation and Design Methodology, Volume 1: Simulation Methodology, Design Applications, and TORMIS Computer Code”, NP-2005-V1,1981.
[8] EPRI, “Tornado Missile Simulation and Design Methodology, Volume 2: Model Verification and Database Updates”, NP-2005-V2, 1981.
[9] Hope, K.D., Povroznyk, N. and Schneider, R., “Tornado Missile Strike Calculator: An Excel-based Stochastic Model of Tornado-Driven Missile Behaviour for Use in High Winds PRA”, International Topical Meeting on Probabilistic Safety Assessment and Analysis (PSA 2015), Sun Valley, Idaho, USA, April 26-30, 12086, 2015.

[10] Goodman, J. and Koch, J. E., "The Probability of a Tornado Missile Hitting a Target", Nuclear Engineering and Design, **74**, pp.125-155, 1983.
[11] Goodman, J. and Koch, J.E., "The assessment of tornado missile hazard to nuclear power plants", Int. Conf. on Numerical Methods in Nuclear Engineering, Montreal, Quebec (Canada), pp.416-429, 1983.
[12] Goodman, J. and Koch, J. E., "Conditional Probability of the Tornado Missile Impact Given a Tornado Occurrence", Proceedings of International ANS/ENS Topical Meeting on Probabilistic Risk Assessment, Vol. I, pp 419-424, Port Chester, New York, 1981.
[13] Eguchi, Y., Murakami, T., Hirakuchi, H., Sugimoto, S. and Hattori, Y., "An Evaluation Method for Tornado Missile Strike Probability with Stochastic Correlation", Nuclear Engineering Technology, **49**, Issue 2, pp.395-403, 2017.
[14] Eguchi, Y., Sugimoto, S., Hattori, Y., Murakami, T., and Hirakuchi, H., "An Estimation Method for Tornado Missile Strike Probability under Assumption of Statistically Isotropic Tornado Path Directions", pp.241-246, Proc. of 2017 International Topical Meeting on Probabilistic Safety Assessment and Analysis (PSA 2017), Pittsburgh, USA, 2017.
[15] Hirakuchi, H., Nohara, D., Sugimoto, S., Eguchi, Y. and Hattori, Y., "Development of a tornado wind speed hazard model for limited area (TOWLA) for nuclear power plants at a coastline", CRIEPI report O15005 (in Japanese), 2016.
[16] Twisdale, L.A. and Vickery, P.J., "Comparison of Debris Trajectory Models for Explosive Safety Hazard Analysis", 25th DoD Explosive Safety Seminar, Anaheim, California, 1992.
[17] Maruyama, T., Kawai, H., Okuda, Y. and Nakamura O., "Numerical Study on Characteristics Debris in Tornado", Annuals of Disaster Prevention Research Institute, 57(B), 248-259. (in Japanese), 2014
[18] Hall, R. T., "Aerodynamic considerations on the injection of tornado-generated missiles from ground level into tornado flow fields", NUREG/CR-0556,1979.
[19] Eguchi, Y., Sugimoto, S., Hattori, Y. and Hirakuchi, H., "Development of TONBOS for simulation of liftoff and flight of objects driven by a tornado", Central Research Institute of Electric Power Industry, Civil Engineering Research Laboratory Report, No. N14002 (in Japanese), 2014.
[20] Eguchi, Y., Sugimoto, S., Hattori, Y. and Hirakuchi, H., "A Rational Method to Evaluate Tornado-Borne Missile Speed in Nuclear Power Plants (Validation of a Numerical Code Based on Fujita's Tornado Model)", Transactions of the JSME, **81**, No.823 (in Japanese), 2015.
[21] Fujita, T.T., "Workbook of Tornadoes and High Winds for Engineering Applications", U. Chicago, 1978. (http://pbadupws.nrc.gov/docs/ML0526/ML052650410.pdf)
[22] Lin, N., "Simulation of windborne debris trajectories", Master of Science thesis, Dept. of Civil Engineering, Texas Tech Univ., Lubbock, Texas, 2005.